

See discussions, stats, and author profiles for this publication at: <https://www.researchgate.net/publication/309965447>

The hygrothermal performance of residential buildings at urban and rural sites: Sensible and latent energy loads and indoor environmental conditions

Article in *Energy and Buildings* · October 2017

DOI: 10.1016/j.enbuild.2016.11.018

CITATIONS

33

READS

788

8 authors, including:



Riccardo Paolini
UNSW Sydney

62 PUBLICATIONS 852 CITATIONS

[SEE PROFILE](#)



Andrea Zani
Politecnico di Milano

12 PUBLICATIONS 105 CITATIONS

[SEE PROFILE](#)



Maryam Meshkiniya
Politecnico di Milano

7 PUBLICATIONS 38 CITATIONS

[SEE PROFILE](#)



Veronica Lucia Castaldo
Università degli Studi di Perugia

62 PUBLICATIONS 1,066 CITATIONS

[SEE PROFILE](#)

Some of the authors of this publication are also working on these related projects:



Overheating in buildings [View project](#)



ELASTOCALORIC COOLING FOR BUILDINGS AND THE BUILT ENVIRONMENT [View project](#)

The hygrothermal performance of residential buildings at urban and rural sites: sensible and latent energy loads and indoor environmental conditions

Riccardo Paolini^{1,*}, Andrea Zani¹, Maryam MeshkinKiya¹, Veronica Lucia Castaldo^{2,3}, Anna Laura Pisello^{2,3}, Florian Antretter⁴, Tiziana Poli¹, Franco Cotana^{2,3}

Accepted for publication in

Energy and Buildings

<http://dx.doi.org/10.1016/j.enbuild.2016.11.018>

©2016. This manuscript version is made available under the CC-BY-NC-ND 4.0 license

<http://creativecommons.org/licenses/by-nc-nd/4.0/>

Disclaimer

This document was prepared as an account of work sponsored by Italian Ministry for Education, University and Research (MIUR). While this document is believed to contain correct information, neither the Italian Government nor any agency thereof, nor the Research Institutions to which the authors are affiliated, nor any of their employees, makes any warranty, express or implied, or assumes any legal responsibility for the accuracy, completeness, or usefulness of any information, apparatus, product, or process disclosed, or represents that its use would not infringe privately owned rights. Reference herein to any specific commercial product process, or service by its trade name, trademark, manufacturer, or otherwise, does not necessarily constitute or imply its endorsement, recommendation, or favoring by the Italian Government or any agency thereof, or the Research Institutions to which the authors are affiliated. The views and opinions of authors expressed herein do not necessarily state or reflect those of the Italian Government or any agency thereof, or their Research Institutions.

¹ Politecnico di Milano, Department of Architecture, Built environment and Construction engineering, Via Ponzio 31, 20133 – Milan, Italy

² CIRIAF — Interuniversity Research Center on Pollution and Environment “M. Felli”, University of Perugia, via G. Duranti 63, 06125 Perugia, Italy

³ Department of Engineering, University of Perugia, via G. Duranti 93, 06125 Perugia, Italy

⁴ Fraunhofer Institute for Building Physics, Department of Hygrothermics, Fraunhoferstr. 10, 83626 Valley, Germany

* Corresponding Author:

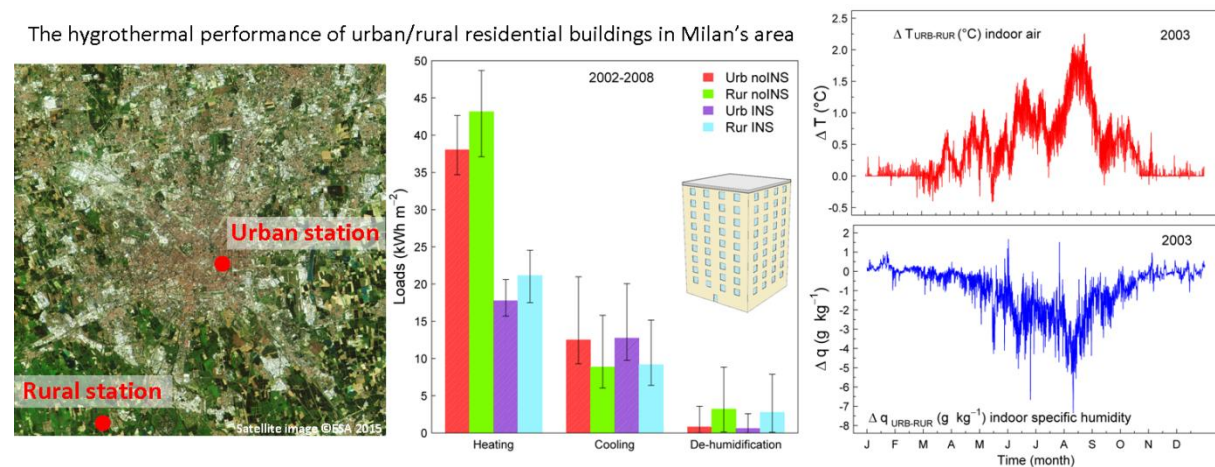
Riccardo Paolini, Email: riccardo.paolini@polimi.it – Address: Via Ponzio 31, 20133 Milan, Italy – Tel. +390223996015

Abstract

Cities often show nighttime air temperatures higher by 3-4 °C than adjacent non-urban areas. This yields to cooling loads in average higher by 13% for urban than rural buildings. Here we assess the hygrothermal performance and the heating and cooling loads of a reference building representative of the Italian stock. We compare its performance calculated with hourly urban weather data (2002-2008) with the performance of the same building using a rural dataset instead. Milan's Urban Heat Island reduces the heating loads by 12% and 16%, for the non-insulated and insulated building, respectively, while the cooling loads are increased by 41% and 39%. The urban building also shows dehumidification loads 74-78% lower than the rural building. Moreover, during the 2003 heat wave, the indoor air temperature is computed to be 1.5 °C-2.2 °C higher in a non-conditioned urban building than in the rural one. This increases the wakefulness, occupants' vulnerability to overheating, and impacts the overall hygrothermal performance. Our findings highlight the need of a different design concept for urban with respect to non-urban buildings, even though they are, by law, in the same climate zone.

Key Words: Urban Heat Island; Building energy simulation; heating; cooling; moisture.

Graphical Abstract



Highlights

- We simulated the heat & moisture balance of a residential building in Milan, Italy.
- We used weather data from 2002 to 2008 collected by a rural and an urban station.
- The UHI reduces heating loads by 12-16% and increases cooling loads by 39-41%.
- Dehumidification loads are 74-78% lower for the urban than for the rural building.
- During heat waves, mortality increases with body overheating and wakefulness.

1. Introduction

As the growth of world's population mostly concerns urban areas, which are responsible for 71% of global energy-related carbon emissions [1], zero energy and healthy communities are nowadays a key target. Therefore, a robust understanding and description of the microclimates where most of buildings are located is necessary, as demonstrated by the increasing number of studies on Urban Heat Islands (UHIs) and their impacts [2,3].

Urbanization is known to induce local climate change phenomena [4]: urban areas present higher air temperatures than their rural proximities, especially during the night [5], often by 3-4 °C, with higher peak differences, sometimes exceeding 10 °C [3]. For instance, in London, a maximum daytime Urban Heat Island Intensity (UHII) of 8.9 °C was found in a semi-urban area during a partially cloudy period, while a maximum nocturnal UHII of 8.6 °C was found in the urban area in clear sky conditions with wind velocity below 5 m s⁻¹ [6,7]. In Athens, UHIIs from 2.7 °C up to 10 °C are reported by studies using data from dedicated meteorological stations [8]. UHIs determine a higher number of extreme hot nights at an urban location than at a rural site, which is expected to be exacerbated by global climate change [4], likely increasing the mortality during heat waves [9].

Metropolitan areas present also lower humidity than non-urban adjacent zones [10], with monthly average differences in relative humidity exceeding 10% [11], although some short duration events of urban moisture excess may occur [12]. Moreover, the wind velocity within the urban canopy is a fraction of that over the rooftops [13], in the range of one fourth to one third [14]. In addition, at 1.5-2 m above the street level the air temperature is about 1-3 °C warmer than over the urban canopy layer [15]. Also rainfalls are affected by the urban texture: precipitations can be increased downwind, slightly increased over the city, and reduced upwind in the rural surroundings [16].

Each city has its specific features which result in different UHIs [2]. An interesting case study is that of Milan, Italy. Its metropolitan region is populated by ~ 7.4 million people [17], with an average urban population density of ~ 7400 people/km², and exceeding 15000 people/km² in the semi-central wards of the city [18]. The first study on Milan's UHI is that by Bacci and Maugeri [19], who report a yearly average UHII exceeding 1.2°C relative to the period 1951-1981, and found a positive correlation between UHII increase and increase in the average radius of the city from 1850 to 1981. Anniballe et al. [20], by means of satellite remote sensing, found an urban-rural surface temperature difference of 9-10 °C during daytime and about 50% less during nighttime within Milan's urban fabric.

Despite the vast literature on the topic, as yet, building energy simulations (BES) are often performed with old weather datasets, mainly collected by weather stations located at the airports. With urban weather data instead of a rural reference, the cooling loads are in average 13% higher, and for each 1 °C of UHII the cooling load is increased by 20% [3]. For a tertiary building in Modena, Italy, Magli et al. computed higher heating primary energy needs outside the city by 19-20%, lower cooling primary energy needs by 8-10%, and lower CO₂ equivalent emissions by 5-7% [21]. Considering instead the overheating risk, although dwelling features and users' behavior are the determinant factors in the exposure to the heat risk, the UHI draws the spatial variation [22]. While the general trend for typical buildings in a given region can

fairly estimate the exposure to overheating, modeling specific dwellings remains challenging. A comparison between EnergyPlus simulations and measurements in 823 dwellings in the UK has shown an average RMSE of 2.7 °C for the indoor maximum daily temperature [23].

In this paper we show the analysis of hourly weather data series (2002-2008) collected at an urban station in Milan, and at a rural one. With these, we computed the heating, cooling, humidification and dehumidification loads, as well as the overheating and over-drying risk (i.e., too low humidity) for a representative residential building. Moreover, we considered the conditions that induce wakefulness and reduce sleep efficiency, the transmission of bacteria, viruses, and respiratory infections, as well as the proliferation of house mites. We gave special attention to the indoor conditions during the heat wave of 2003, when in Milan the mortality increased by 23% over the 1995-2002 average, corresponding to 559 deaths in excess [24].

2. Method

2.1. Simulation model

We computed the whole building (3-D) dynamic heat and moisture balance using the software model WUFI Plus 3.0.3 [25]. It resolves the enthalpy balance with the finite control volumes method, coupling heat transfer with liquid and vapor moisture transport in porous media, accounting for latent heat transformations as well as for temperature and moisture dependent thermal and moisture transport properties [26]. Wind driven rain is also considered. WUFI Plus was validated within the context of IEA Annex 41 [27], and tested with measurements in the laboratory and experimental buildings [28–30]. For a residential building in Quebec City (Canada) and Phoenix (AZ, USA), Ge and Baba found a difference within 2.7% between the heating and cooling loads computed with WUFI or EnergyPlus [31].

2.2. Case study

As a case study, we selected a typical residential building, based on a survey of Milan's building stock [32]. It is a stand-alone ten-story tower building, representative of the 1961-1975 housing stock [33]. Being an isolated building, thus not surrounded by urban canyons, there are no significant obstructions around it that may influence the radiative and convective exchanges. The dimensions of the selected building equal to 20.3 m × 20.3 m × 30 m with the façades facing the cardinal directions. The net floor area is of 3307 m², and windows of 1.6 m × 1.7 m are on each façade, sized according to local regulations. The same building is simulated in a non-insulated and in a retrofitted condition (Table 1). The non-insulated case presents a building envelope technology representative of multi-story residential buildings in Italy. The refurbished case, instead, complies with the new energy regulation [34], with external wall insulation (ETICS) and an insulated cool roof. The shading coefficient was adjusted to achieve a reduction of solar loads correspondent to the target value of 0.35 for the solar heat gain coefficient as required by the Italian Law [34], as a function of the angle of incidence of solar radiation. Aged values for the roof and wall solar reflectance (ρ_s) and thermal emittance (ε) are experimental results achieved at the same location [35,36]. The capillary water absorption coefficient (A_w) of the exterior wall finish (a 0.002 m thick top coat) is equal to 0.002 kg m⁻² s^{-0.5}: a typical value for exterior finish systems. The opaque

building components (Table 1) were modeled with a mesh of 70 finite control volumes each, namely discretized in layers thinner than 0.01 m. The simulations were initialized with the data of 2006, i.e. the closest to the average of the dataset, and then run with hourly time step from 1st January 2002 to 31st December 2008.

Table 1. Building envelope characteristics and surface areas used for the simulations.

Building components	Orientation and area (m ²)	Case 1: No insulation	Case 2: Insulated building
Wall	Tot. 2014 N: 503.5 E: 503.5 S: 503.5 W: 503.5	$U = 0.49 \text{ W m}^{-2} \text{ K}^{-1}$ 0.015 m Cement lime plaster, Double hollow-brick masonry with air gap (0.08 m – 0.05 m – 0.12 m), 0.015 m cement plaster and finish coat. $\rho_s = 0.50$; $\varepsilon = 0.90$	$U = 0.22 \text{ W m}^{-2} \text{ K}^{-1}$ 0.015 m Cement lime plaster, Double hollow-brick masonry with air gap (0.08 m – 0.05 m – 0.12 m), ETICS with 0.1 m EPS insulation. $\rho_s = 0.50$; $\varepsilon = 0.90$
		$U = 0.56 \text{ W m}^{-2} \text{ K}^{-1}$ 0.015 m Cement lime plaster, 0.25 m precast reinforced concrete slab, 0.08 m slope screed, 0.05 m concrete screed and modified bitumen roofing felt. $\rho_s = 0.25$; $\varepsilon = 0.90$	$U = 0.23 \text{ W m}^{-2} \text{ K}^{-1}$ 0.015 m Cement lime plaster, 0.25 m precast reinforced concrete slab, 0.08 m slope screed, 0.05 m concrete screed, 0.1 m EPS insulated panel, cool PVC roof membrane ($\rho_s = 0.56$; $\varepsilon = 0.90$)
Roof	412	$U = 0.51 \text{ W m}^{-2} \text{ K}^{-1}$ 0.015 m Cement lime plaster, 0.25 m precast reinforced concrete slab, 0.05 m concrete screed and 0.008 m granite finishing	$U = 0.51 \text{ W m}^{-2} \text{ K}^{-1}$ 0.015 m Cement lime plaster, 0.25 m precast reinforced concrete slab, 0.05 m concrete screed and 0.008 m granite finishing
Floor	412/ Tot. 3709	$U = 0.52 \text{ W m}^{-2} \text{ K}^{-1}$ 0.25 m precast reinforced concrete slab, 0.05 m concrete screed and 0.008 m granite finishing	$U = 0.29 \text{ W m}^{-2} \text{ K}^{-1}$ 0.015 m Cement plaster, 0.06 m EPS insulated panel, 0.25 m precast reinforced concrete slab, 0.05 m concrete screed and 0.008 m granite finishing.
Floor over cellar	412	$U = 0.52 \text{ W m}^{-2} \text{ K}^{-1}$ 0.25 m precast reinforced concrete slab, 0.05 m concrete screed and 0.008 m granite finishing	$U = 0.29 \text{ W m}^{-2} \text{ K}^{-1}$ 0.015 m Cement plaster, 0.06 m EPS insulated panel, 0.25 m precast reinforced concrete slab, 0.05 m concrete screed and 0.008 m granite finishing.
Window	Tot. 418.5 N: 108.8 E: 106 S: 97.92 E: 106	$U = 2.85 \text{ W m}^{-2} \text{ K}^{-1}$ Frame factor = 0.8 g-value = 0.75 Standard double glazing unit + external venetian blinds	$U = 1.4 \text{ W m}^{-2} \text{ K}^{-1}$ Frame factor = 0.8 g-value = 0.57 Double glazing unit with low emissivity coating + external venetian blinds

2.3. Outdoor boundary conditions

The outdoor climate data used in this study were collected from 2002 to 2008 by two weather stations of the network of ARPA Lombardia [37]: Milano Juvara, within the city

centre, and Lacchiarella, approximately 18 km further south (12 km from the city boundaries). Both stations provide hourly averages of ambient temperature (T_{ext}) and relative humidity (RH_{ext}), wind velocity and direction, global horizontal solar radiation, air pressure, and rainfall, while the diffuse solar radiation and the long-wave incoming radiation were modeled [38,39].

When using raw data measured by weather stations, encountering missing values is inevitable [40] (our raw data show a maximum of 3.4% gaps for the urban T_{ext}). To fill these gaps and control the spatial consistency of the measured quantities, we used a multilayer perceptron (MLP) [41], which in our case is a Back-Propagated Neural Network (BPNN) trained by using the Levenberg-Marquardt algorithm. The perceptron replicates the relation between other climatic observations at nearby weather stations, seven in our case, with the target stations, namely Juvara and Lacchiarella (Figure 1).

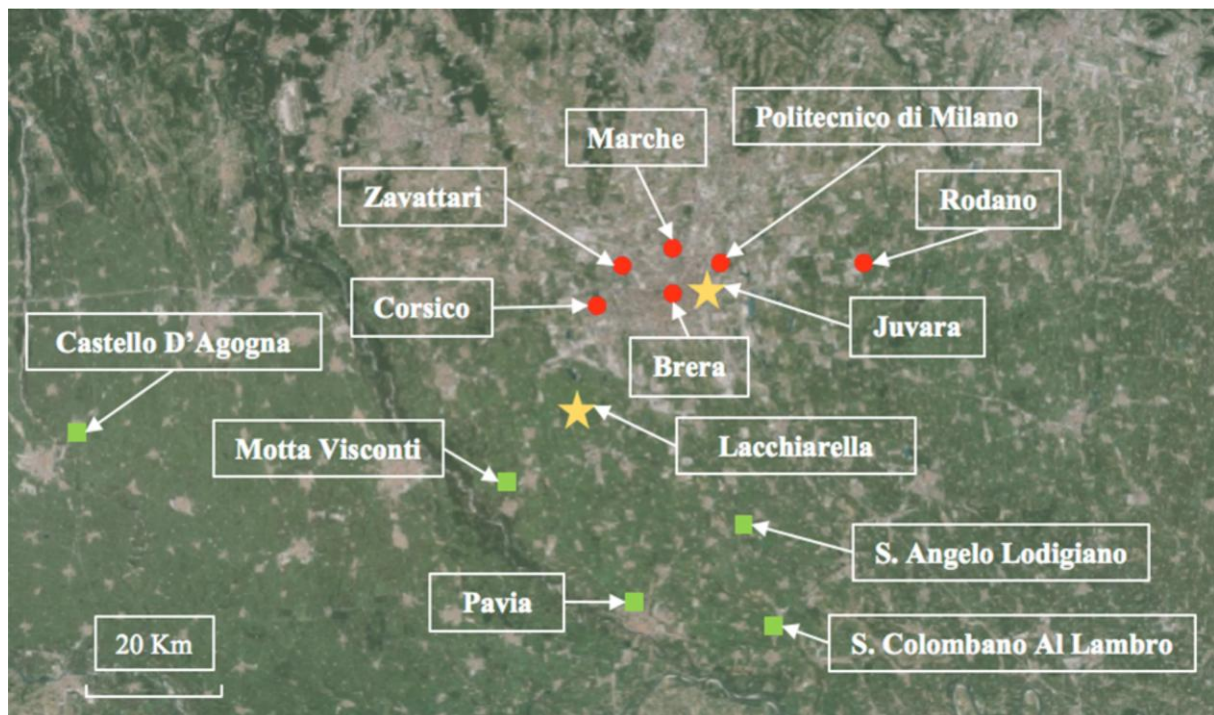


Figure 1. Network of stations. The yellow stars identify the target stations (i.e., the stations used as backbones), the red circles are the stations used to feed the BPNN for T_{ext} and RH_{ext} , while the green squares identify the stations used for spatial consistency tests and gap filling of wind speed and velocity, solar radiation, and rainfall.

We applied this procedure on the missing observations of T_{ext} and RH_{ext} , and we performed quality tests on the infilled data, with the thresholds for the general range tests identified by Estevez et al. [42], and relation tests with site specific thresholds for Milan's context (Table 2). The latter are the 99.9th percentiles of the hourly variations for the period 2011-2015 from a weather station (Vaisala WXT 520) in Politecnico di Milano, managed by the Osservatorio Meteo Milano Duomo [43]. Then, we performed validation, spatial consistency, range, and relation tests on all measured quantities.

Table 2. Range test and relation test thresholds.

Test	Quantity	Threshold
Range test	Relative Humidity (RH)	$10\% \leq RH \leq 100\%$
	Temperature (T)	$-20^\circ\text{C} \leq T \leq 50^\circ\text{C}$
Relation test	Relative Humidity (RH)	$ \text{RH}_h - \text{RH}_{h-1} \leq 18.8\%$
	Temperature (T)	$ T_h - T_{h-1} \leq 3.85^\circ\text{C}$
	Wind Speed (WS)	$ \text{WS}_h - \text{WS}_{h-1} \leq 2.3 \text{ m s}^{-1}$

Over seven years, the median UHII is of 1.1°C , with the interquartile range comprised between 0°C and 2.7°C , and for 5% of the time the UHII is greater than 5°C , while the absolute UHII peak is of 12.2°C during the winter of 2003 (Figure 2a). The maximum UHIIs occur almost always during the heating season, while some cool islands phenomena take place during the intermediate and cooling season. For most of the time the urban area shows lower specific humidity than the rural surroundings (Figure 2b). The interquartile range is comprised between -1.44 and -0.27 g kg^{-1} , with a median of -0.67 g kg^{-1} , while for less than 10% of the time the city is moister than the non-urban adjacent area.

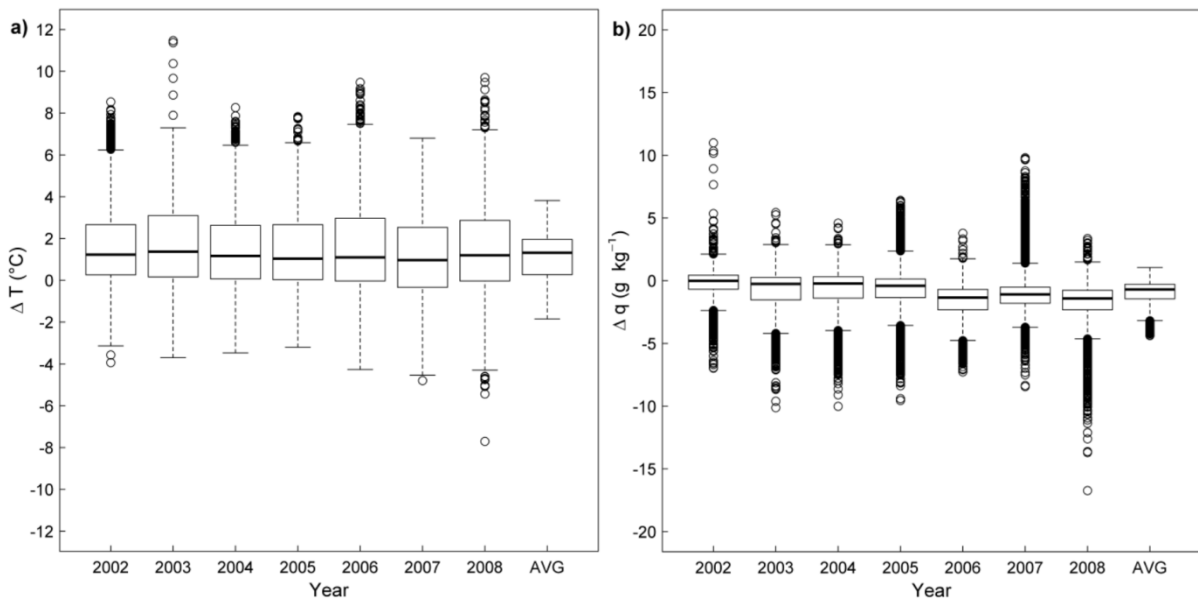


Figure 2. Difference between urban and rural (a) T_{ext} and (b) specific humidity, computed considering the simple moving averages over three hours.

Finally, the seven-year average rainfall is of 785 mm at Milano Juvara and of 731 mm at Lacchiarella, with documented strong spatial differences, even of 300 mm, during rainy years [37,44]. However, the wind velocity in Milan's area is typically low (in average $\sim 1.5 \text{ m}^{-1}$), and thus the integral of wind driven rain in all directions does not show strong spatial variability ($\leq 60 \text{ mm y}^{-1}$), while the main direction is affected. Trees and other buildings, rain type and angle of incidence may induce larger differences in the absorption of wind driven rain [45,46].

2.4. Indoor boundary conditions

We assumed the internal specific heat and moisture loads from the literature and standards [47,48], and we computed the occupancy factor after the survey by Papakostas and Sotiropoulos [49] (Table 3). Starting from the ranges and duration for the events that lead to moisture generation (e.g., meal preparation, showers, etc.) [48], we defined three moisture load scenarios (Table 4). Table 5 details the set points for the building services.

Table. 3. Occupancy and internal heat gains and moisture sources. *Other moisture loads consider different people activities and small events like bath and cleaning **Clothes drying loads were distributed during evening and night hours.

Occupancy and internal heat and moisture loads						
Time	F _d (occupancy factor)	N° of occupants	Heat loads (W m ⁻²)	Moisture loads/ person (g h ⁻¹ p ⁻¹)	Other Moisture loads (g h ⁻¹)*	Events
7:00 - 9:00	0.62	81	6	50	100	Shower (220 g h ⁻¹ per person), Breakfast (200 g h ⁻¹ per family)
9:00 - 17:00	0.27	35	6	90	100	Lunch (300 g h ⁻¹ per family)
17:00 - 19:00	0.62	81	13	90	100	-
19:00 - 21:00	0.96	125	13	90	100	Dinner (635 g h ⁻¹ per family)
21:00 - 23:00	0.96	125	13	90	100	Dishwasher (310 g h ⁻¹ per family)
23:00 - 7:00	0.98	127	3	50	100	Clothes drying (1500 g h ⁻¹ per family)**

Table. 4. Total specific moisture loads in the three moisture generation scenarios.

Total specific moisture loads (g h ⁻¹ m ⁻²)			
Hours	Low	Normal	High
7:00 - 9:00	5.3	7.1	11.2
9:00 - 17:00	1.5	2.2	2.4
17:00 - 19:00	3.2	4.6	5.6
19:00 - 21:00	7.7	11.5	15.2
21:00 - 23:00	5.3	10.7	14.4
23:00 - 7:00	2.5	2.7	2.9

Table. 5. Building services and set points.

Heating	$T = 20^{\circ}\text{C}$
Cooling	$T = 26^{\circ}\text{C}$
Humidification	$\text{RH} \geq 20\%$
Dehumidification	$\text{RH} \leq 70\%$

With regard to the air change rates per hour (ACH), first we computed the daily mean (\overline{ACH}) as the maximum between the correlation given by ISO 13788 [50] and a minimum threshold [51]:

$$\overline{ACH} = \max(0.2 + 0.04 \cdot \overline{T}_{ext}; 0.5) \quad (1)$$

where \overline{T}_{ext} is the daily mean of the outdoor air temperature. The hourly ACH is the product between \overline{ACH} and an hourly distribution for winter and summer conditions [52], including natural ventilation and infiltrations/exfiltrations rates (Figure 3), suited for residential buildings [53]. We computed the rain load on the façades corresponding to 24% of the wind driven rain [54] at 15-20 m, with medium exposure and walls subject to runoff. Finally, we set ρ_s and ε of the surroundings equal to 0.15 and 0.90, respectively.

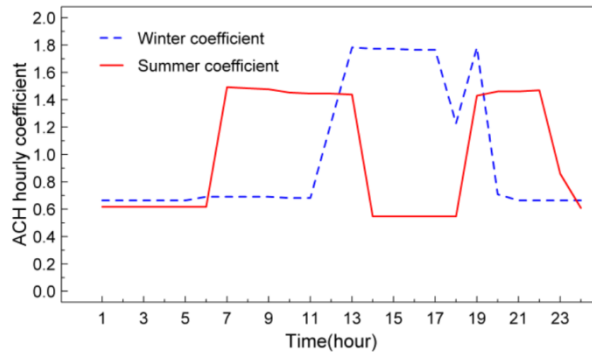


Figure 3. Winter and summer hourly ACH coefficient (i.e., hourly value / daily mean).

2.5. Descriptors of the indoor environmental performance

To assess the difference between the simulated and the target indoor thermal conditions, we used the building Thermal Deviation Index (TDI_b) [55]. Considering here a specific analysis focused on summer conditions, TDI_b describes the frequency and the intensity of the gap between the target and the measured/computed indoor operative temperature (T_{op-in}) in the middle of the thermal zone. TDI_b is then calculated as follows (2):

$$TDI_b = \frac{\int_{P_h} |T_{op-in} - 26| d\tau + \int_{P_c} |23 - T_{op-in}| d\tau}{TDI_{BC}} \frac{t_s - t_{T-s}}{t_s} \quad (2)$$

where 26 and 23 (in $^{\circ}\text{C}$) are, respectively, the maximum and minimum acceptable ranges for T_{op-in} for the cooling season, as defined in EN 15251 [53], t_s is the period of the analysis and t_{T-s} is the period when T_{op-in} is within the thermal target range. P_h and P_c are

the integration domains, when T_{op-in} is out of the defined target. Finally, TDI_{BC} is the arbitrary base case scenario represented by a constant T_{op-in} , i.e. 3 °C far from each thermal target.

Although several thermal comfort indices were validated for indoor environments [56,57], here we consider the Humidex index [58], as it is used in epidemiologic studies on the extra-mortality during the 2003 heat wave in Northern Italy [59,60]. Other descriptors concern the conditions that increase wakefulness and low quality sleep (computed only for the summer of 2003), favorable conditions to house mites [61], and the conditions that favor the transmission of bacteria, viruses, respiratory infections, and that promote dryness of skin and mucous membranes (Table 6). Low sleep efficiency and increased wakefulness are counted when both the specific humidity exceeds that at the temperature and relative humidity values at which the sleep efficiency studies were performed [62], and the indoor temperature the threshold of 29°C [63]. To compare the indoor hygrothermal performance in the different considered scenarios, we counted the hours when the defined thresholds are trespassed.

Table 6. Risk conditions with regard to bacteria, viruses and respiratory infections transmission, dry skin, sleep efficiency and wakefulness.

Condition	Threshold/Interval	Reference
Favored bacteria transmission	RH \leq 30%; RH \geq 60% (@23°C)	[64]
Favored viruses transmission	RH \leq 50%; RH \geq 70% (@23°C)	[64]
Favored respiratory infections transmission	RH \geq 70% (@23°C)	[64]
Mortality of house mites during development phase	Regression from experimental data (eq. (13) and (14))	[61]
Dry skin / mucous membranes	RH \leq 30% (@23°C)	[64]
Low sleep efficiency	T = 35°C; RH = 50%	[62]
Increased wakefulness for tropical nights	T \geq 29°C	[63]

3. Results and discussion

3.1. Heating, cooling, humidification, and dehumidification loads

A non-negligible and systematic inter-annual variability is detected across the simulated period (i.e., 2002-2008), both in terms of heating and cooling loads (Figure 4a,b). The rural scenarios show always higher heating loads both with and without insulation compared to the urban scenarios (Figure 4a). Considering the specific loads referred to the net floor area, the peak rural-urban difference is of 8.1 and 4.8 kWh m⁻² y⁻¹ in 2002 for the non-insulated and insulated envelope configurations, respectively. In average, the differences account for 5.1 and 3.4 kWh m⁻² y⁻¹, for non-insulated and insulated buildings, corresponding to 12% and 16% of the rural heating load.

On the contrary, always lower cooling loads are computed in the rural scenario with respect to the urban one, almost irrespective of the presence of building insulation (Figure 4b). This is not surprising as the solar heat gains through the transparent envelope are mainly controlled by the shading devices. Thermal insulation, in average, reduces the heating loads

by approximately $20 \text{ kWh m}^{-2} \text{ y}^{-1}$ within the metropolitan area, and by $22 \text{ kWh m}^{-2} \text{ y}^{-1}$ in the rural surroundings, while it slightly increases the cooling loads (with a small reduction only in 2003), without relevant urban-rural differences. The maximum gap between the urban and rural scenarios is equal to 5.2 and $4.9 \text{ kWh m}^{-2} \text{ y}^{-1}$ (in 2003) for the non-insulated and insulated envelope configurations, respectively. The difference for the seven-year average is of $3.6 \text{ kWh m}^{-2} \text{ y}^{-1}$, which is 39-41% of the cooling load for the rural building.

A larger reduction of the heating needs compared to the increase in cooling needs due to the UHI is not surprising, considering the prevalence of peak UHIIs during winter, as previously discussed. Moreover, the reduction in heating loads thanks to insulation is slightly larger (i.e., by $1.7 \pm 1.4 \text{ kWh m}^{-2} \text{ y}^{-1}$) for a rural building compared to the urban one. Focusing on the variability from 2002 to 2008, the half range is 10-14% of the heating loads of the urban building, while it is of 13-17% for the rural case. Therefore, the urban fabric seems to dampen the inter-annual variability in heating needs. On the contrary, the cooling loads show very large inter-annual variability, with a half range of 40-47% of the average cooling needs for the urban building and 48-55% for the rural one.

This is largely due to the climate anomaly of the summer of 2003, when a heat wave impacted Continental Europe, with several weeks characterized by outdoor air temperatures above 35°C [60]. In fact, excluding 2003, the ratio between the half-range and the average cooling load is of 15-17% in the urban area, and of 22-24% for the rural building. Considering an extreme year such as 2003, the cooling load of the urban building is 2.3 times larger than the average for the rural building. The use of design years for hot summers, instead of typical meteorological years, has been previously addressed as a better option for cooling loads and ventilation analyses [40]. However, we argue that using a whole data series could provide relevant information for decision making about the building envelope design and building services, not just in terms of sizing, but also in terms of flexibility in use and design of the response to climate anomalies. Using whole data series can be particularly important for heat and moisture balance analyses.

In average, the dehumidification load at the rural site is roughly three times that within the urban area, and it is one third of the cooling load with a normal moisture load, and half of the cooling load with high indoor moisture generation (Figure 4c). However, during moist years, the dehumidification loads of rural buildings can be as much as the cooling loads (with a set point at 70% relative humidity), and of a magnitude greater than the dehumidification loads of urban buildings. Small humidification loads – in the range of one thousandth of the dehumidification loads – are computed only for urban buildings only during very dry years (Figure 4d), specially with low indoor moisture generation. Higher insulation levels induce higher indoor air temperatures also during the intermediate season, and therefore slightly lower dehumidification loads and higher humidification loads with the same moisture loads.

Since we selected a wall finishing with a low water absorption coefficient, the heating loads of the non-insulated building with and without driving rain differ by less than 0.5%. Therefore, with the considered building envelope, urban-rural differences concerning the heating, cooling, and dehumidification loads due to this aspect are negligible.

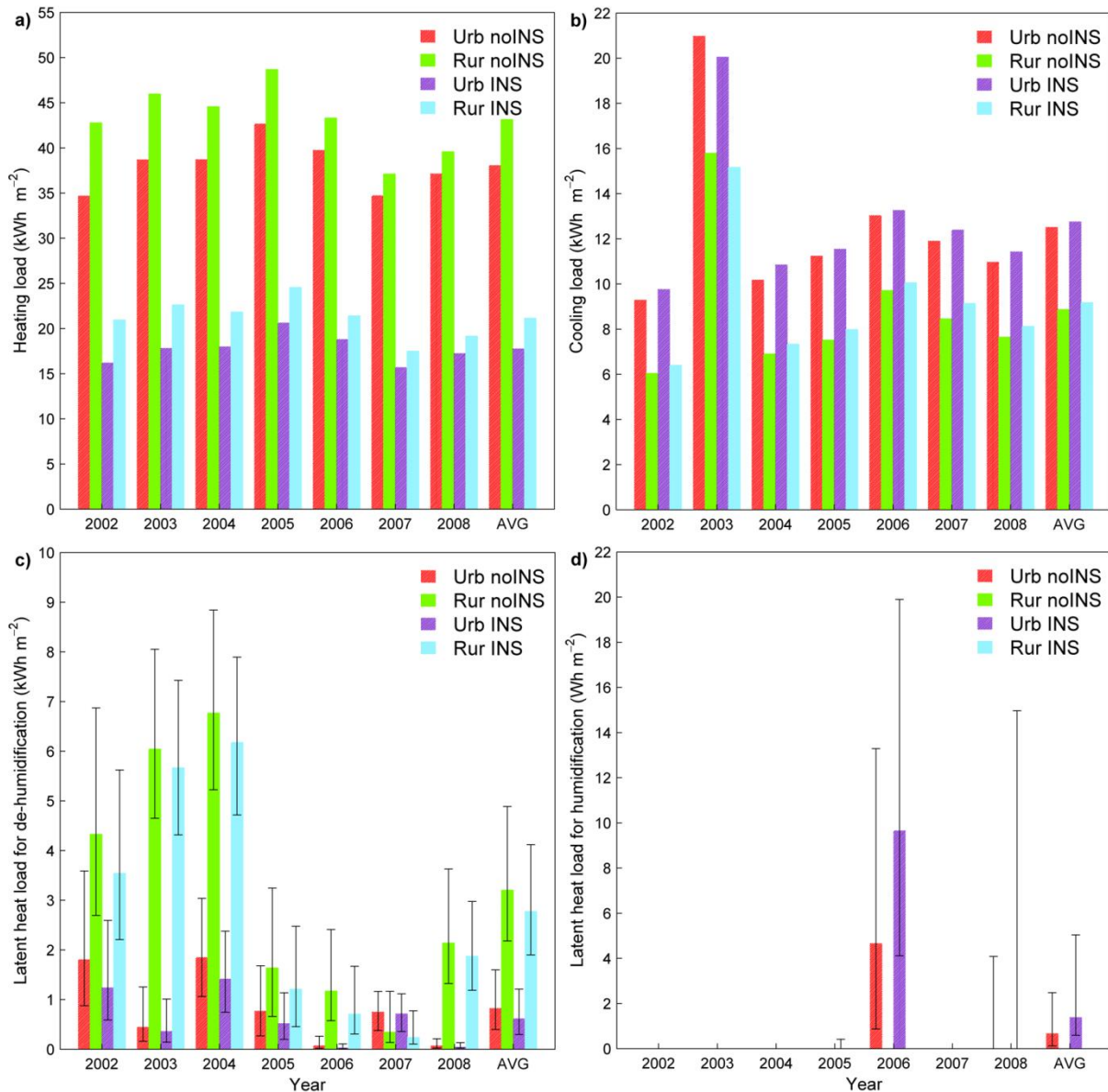


Figure 4. Heating (a) and cooling loads (b), and latent heat loads for dehumidification (c) and humidification (d) in the different assessed scenarios: urban and rural without envelope insulation, and urban and rural with envelope insulation. Note that the latent heat load for humidification is in Wh m⁻². The whiskers of the error bars indicate the results with low or high indoor moisture loads (as in Table 3).

3.2. Indoor conditions without cooling and humidity services

Without air conditioning, a significant and pseudo-constant difference in the seven-year average indoor air temperature profiles is evident (Fig. 5a). The UHI induces an indoor urban-rural air temperature difference, with peak values of 1.4 °C in non-insulated building and 1.5 °C in the insulated case, up to 2.2 °C and 2.3 °C during 2003 (Figure 5b). While the persistence of the absolute difference is interesting, the frequent peak values of the indoor air temperature isolate the issues: during 2003 the 95th percentile of the indoor air temperature of the urban building is of 31.5-32.5 °C, while it is of 30.3-30.9 °C for rural buildings (the higher values relate to the insulated scenario).

Considering the heating season (15th Oct – 15th Apr), the differences between the seven-year average peak indoor air temperatures are of 0.6 °C for insulated buildings and negligible in the non-retrofitted scenario. During the intermediate season (Apr 15th – May 31st, Sept 1st – Oct 15th), instead, the peak values differ by 0.8 °C and 1 °C for the non-insulated and insulated cases, respectively. This indicates an overheating risk already during the intermediate season, when the set point for cooling, i.e., 26 °C, is trespassed for 28% of the time in insulated urban buildings, and 17% of the time in rural ones. During hot years like 2003, in urban buildings the air conditioning would be necessary for 40% of the time already during the intermediate season (23% in the rural area). Considering the whole dataset, with a set point for cooling equal to 26 °C, in urban insulated buildings the air conditioning would be operating for 31% of the time, and 284 more hours per year (in average) than at a rural site.

The most significant differences between the urban and rural indoor conditions relate to the moisture levels (Figure 5c,d). With a medium moisture generation, the urban buildings, insulated or not, show a systematically lower seven-year average indoor specific humidity than the rural ones, with the maximum differences exceeding 3.5 g kg⁻¹ in summer.

This difference exceeds 7 g kg⁻¹ during the hot summer of 2003. Although the absolute values are different, the differences between urban and rural buildings are roughly the same in all moisture generation scenarios (within 0.2 g kg⁻¹). Between high and low moisture loads scenarios, at the same location, the differences account for 2.2-2.5 g kg⁻¹ during the heating season, and for 0.8-0.9 g kg⁻¹ in summer. Therefore, for the analyzed cases, the uncertainty in the outdoor boundary conditions described by microclimate around a specific building may prevail over the uncertainty in the indoor moisture loads during the intermediate season and summer. This can be explained considering that *ACH*, in our case, approaches 2 during the cooling season.

Usually, high indoor moisture levels are associated with mould growth risk, but in our case we computed low probability of biological growth with Sedlbauer's model, considering the indoor surface temperature and relative humidity [65]. This is not surprising, as the indoor relative humidity seldom and for short time intervals is greater than 80%. Instead, indoor relative humidity never exceeds 89% for more than one week or 100% for one day, that can be regarded as a quick indicator of mould growth risk, as it is the critical threshold for *Aspergillus versicolor* [66]. In fact, ventilation rates that comply with the indoor air quality standards usually can lower the indoor humidity in a time that is shorter than the minimum time that is necessary for the germination of biological species.

However, mold growth is not the only issue related to unsuited indoor moisture levels [64]. Considering the thresholds summarized in Table 5, we computed a higher risk of bacteria transmission in the rural buildings, similar risk for the transmission of viruses such as that of influenza, and remarkably higher risk of respiratory infections in urban buildings (Figure 6a). Of course, with this metric we just compute the percentage of time when there are favorable conditions to the transmission, but if no bacteria or viruses are present (i.e., no sick person in the dwelling) the risk is anyway zero. As well, also dry skin and mucosal irritation are more likely in urban buildings than in similar buildings in the countryside. Even though the time exceeding the thresholds for mucosal irritation is less than 10% in one year, this may

be sufficient to induce acute symptoms. In fact, approaching 20% of relative humidity, serious hygrothermal discomfort and health risk is reported, in terms of, mucosal irritation, dry eye, ophthalmic pain, and other respiratory symptoms [64,67–69]. Therefore, over-drying of urban buildings could represent a more significant issue than overheating, on which most of the literature focuses.

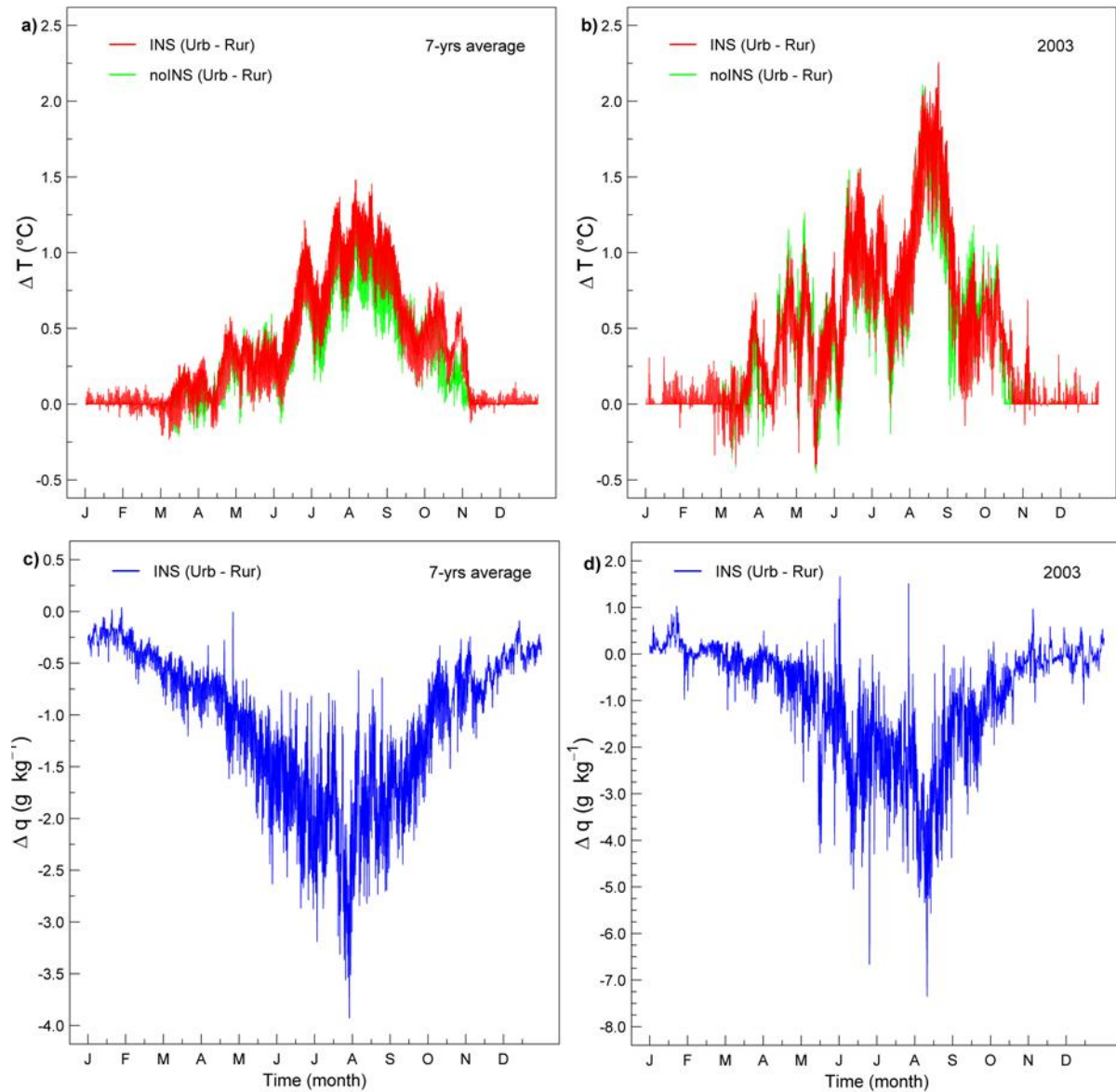


Figure 5. Difference between the urban and rural (a) sever-year average and (b) 2003 indoor air temperature (insulated or not), and (c) sever-year average and (d) 2003 indoor specific humidity (only for the insulated case). The urban-rural differences are computed between the simple moving averages over three hours.

In rural buildings, especially those poorly insulated with intermediate-to-high indoor moisture loads, the mortality of house mites is clearly lower than in urban buildings (Figure 6b). Ucci et al. developed a model to compute the population dynamics of house mites in beds [70], but their model considers vapor diffusion only, and neglects liquid transport and

hygroscopicity, that are relevant for mattresses and beddings. Therefore, we decided to consider only the indoor environmental conditions, as an indicator of the general risk.

All the analyses presented so far are helpful to grasp the general indoor hygrothermal quality, but do not explain another relevant difference between rural and urban dwellers: why the mortality rate, especially for the elderly, is higher in urban than in rural areas during heat waves, predominantly at home [71]. Semenza et al., for the Chicago heat wave of 1995, observed a prevalence in excess deaths for people who lived on the top floor (4.7 times the average of those not living on the top floor) and did not leave home (6.7 times the average of those who left home at least once per week) [72]. Therefore, outdoor conditions seem to be less helpful to understand the extra mortality than the indoor environment, since we spend most of our lifetime indoors, and significant overheating occurs during heat waves.

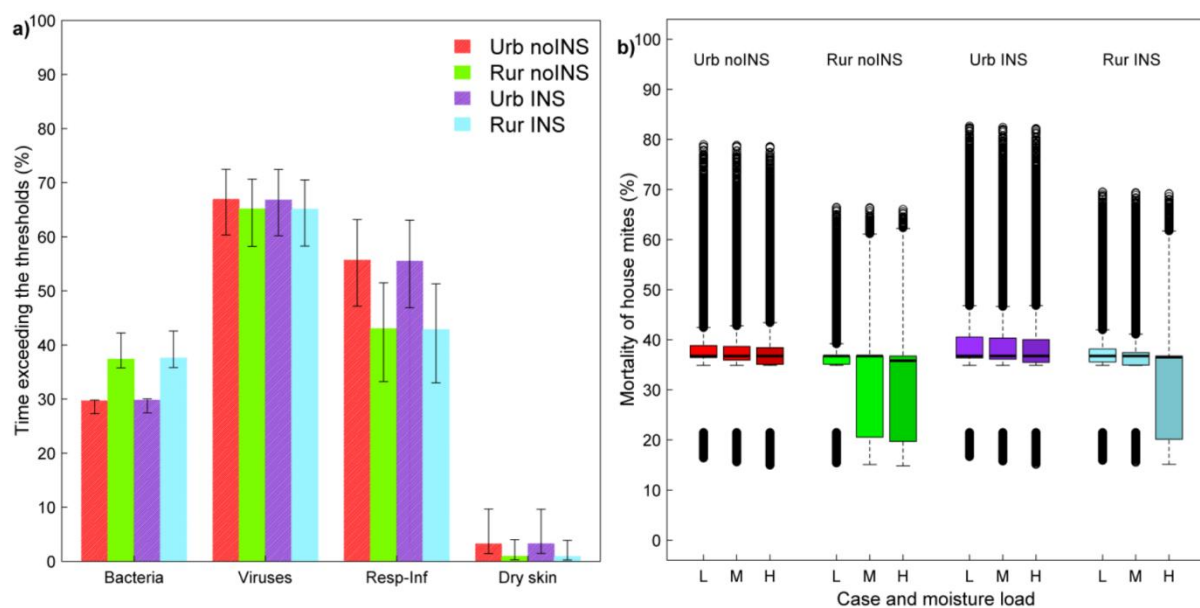


Figure 6. a) Time exceeding the thresholds that identify the lowest risk conditions for bacteria, viruses, and respiratory infections transmission, and dry skin / mucosal irritation; b) mortality of house mites.

Considering only the summertime, we observed that the deviation from the target conditions is more pronounced during the night than during the day (Figure 7). In detail, during the summer of 2003, TDI_b is greater than 0.7 for non-insulated urban buildings, while is of approximately 0.4 for rural building, and in both cases, the summertime TDI_b is roughly double during 2003 than during other years.

Following the metrics used by epidemiologic studies [59], we computed the Humidex index indoors, for urban and rural buildings during the summer of 2003 (Figure 7b). From this analysis would emerge that dangerous conditions prevail in rural buildings, which is in contrast with the observation of higher extra-mortality in urban areas [73]. Moreover, the Humidex, like other thermal stress indices, is a steady state indicator, that does not take into account the accumulation of stress, which is a key factor as revealed by epidemiologic studies [74]. In fact, during the Chicago 1995 heat wave, those who either had operating air

conditioning, or visited other air-conditioned places were less impacted by extra mortality (between 20% and 30% of the average of those who had no access to air conditioning) [72].

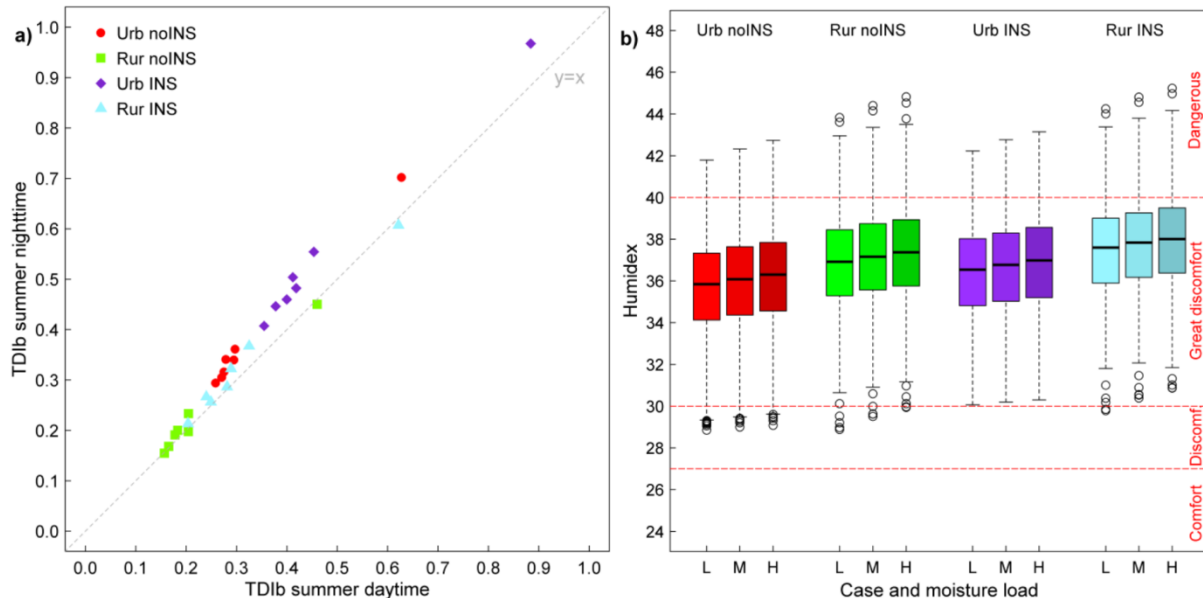


Figure 7. Plots of the Thermal Deviation Index during the summertime (a), and of the humidex index during the summer of 2003 (b).

Since sleep deprivation increases resting blood pressure [75], and “short sleep over a prolonged period may be associated with an increased risk of mortality” [76], although it is not fatal by itself [77], we computed the number of hours when the sleep quality is affected or wakefulness is more likely. Reading the number of deaths in Milan during the summer of 2003 against the hours when sleep quality is likely to be affected, we note a correlation between deaths and prolonged conditions that may impair rest (Figure 8). In urban buildings there is a prevailing number of consecutive hours when wakefulness is likely to be increased, as the indoor air temperature is greater than 29°C [63]. The situation is even worsened with increasing insulation levels. In rural buildings, instead, there seem to be some interruptions offering relief to this sequence of non-resting nights, but tropical night conditions are more frequent, with increased wakefulness due to inefficient transpiration because of high humidity. The sleep efficiency is also reduced for the same reasons. Although high humidity may jeopardize the cooling of a human body by means of transpiration, excessively low humidity may yield to dehydration, and during the Chicago heat wave of 1995, “the majority of excess hospital admissions were due to dehydration”, in addition to heat stroke, and heat exhaustion [78].

Michelozzi et al. [24], for the 2003 heat wave in Milan, report an excess in the deaths due to respiratory issues by 82%, by 68% for metabolic/endocrine gland disorders (that comprise dehydration), and by 118% for illness related to the central nervous system (e.g., Parkinson’s and Alzheimer’s disease). We computed, in fact, a higher fluid loss by respiration and transpiration within urban dwellings (Figure 8b).

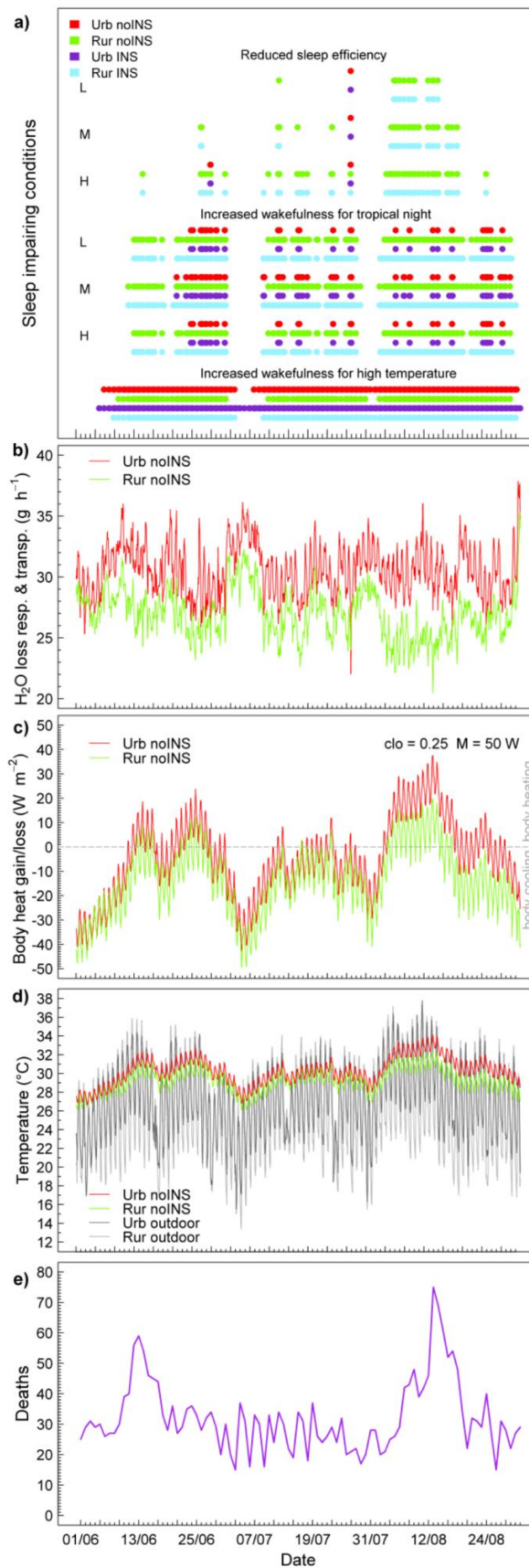


Figure 8. Sleep impairing conditions (a), body moisture loss for respiration and transpiration (b), body heat gain/loss (c), indoor and outdoor air temperatures (d), and mortality in Milan (e) (the latter is re-drawn from [24]).

However, the indicator that seems to better fit with the mortality profile is the heat balance of the human body, here shown for 0.25 clo and 50 W of metabolic activity (Figure 8c). Therefore, when there is heat accumulation even for semi-nude subjects in rest condition, the mortality peaks. There is not a peak in deaths corresponding to the second increase in body heat storage, after the second half of June, and this might be explained by an increase in humidity and lower body fluid losses (Figure 8b), or by a harvesting effect (i.e., the subjects at risk already died during the first event). Comparing the number of deaths (Figure 8e) with the indoor or outdoor air temperatures does not seem helpful to identify the significant thresholds and the reasons of the excess mortality (Figure 8d).

4. Future developments

In this paper, we considered a stand-alone building. The next step is to address the hygrothermal performance of urban buildings located in different urban canyons, considering also the heat and moisture balance of the whole canyon [79,80]. A further area of investigation is represented by the influence of occupancy on the hygrothermal response, as it is known for the energy performance [81–83], and different patterns in users' behavior can be identified in urban or rural dwellings.

5. Conclusions

A vast literature documents the impact of urban heat islands on the building energy performance. However, less information is available about the impacts over long periods and on the hygrothermal performance. In this study we considered a residential stand-alone building representative of the Italian stock, and we performed whole building heat and moisture transport simulations with weather data from 2002 to 2008 collected by a rural and an urban station in Milan, Italy.

Within the city, with respect to the rural case, the heating loads are reduced by 12% and 16%, for a non-insulated and insulated building, respectively, while the cooling loads are increased by 41% and 39%. The urban building also shows dehumidification loads 74-78% lower than for a rural building. During hot years such as 2003, the cooling load of the urban building is 2.3 times larger than the average for the rural building, namely than with the boundary conditions that commonly drive the design of building envelope and services.

In buildings without air conditioning, there is an indoor urban-rural air temperature difference, with peak values of 1.4-1.5 °C (2.2-2.3 °C during 2003). In hot years such as 2003, in urban buildings the air conditioning would be necessary for 40% of the time already during the intermediate season (23% in the rural area), with a set point for cooling of 26 °C. We computed a higher risk of bacteria transmission in the rural buildings, and higher risk of respiratory infections and mucosal irritation in urban buildings, where, instead, house mites are less likely to survive.

During the heat wave of 2003 the mortality rate was found to be correlated to the number of consecutive nights when sleep is impaired because of increased wakefulness. Moreover, we computed a greater fluid loss by respiration and transpiration within urban

dwellings than in rural ones. Considering the body thermal balance, when there is heat accumulation even for semi-nude subjects in rest condition, the mortality peaks.

The key findings of our work outline the need to improve the metrics to assess the impact of hygrothermal conditions on sleep, since existing thermal comfort models are not suited for the purpose. Moreover, they compute lower risk with lower humidity, since they were designed with questionnaires, and human beings are not provided with humidity receptors. We only sense high humidity indirectly, as increased thermal discomfort. This might induce a dangerous bias, especially during heat wave conditions in urban areas, where the air is consistently drier than in the rural proximities. Our findings also highlight the need of different design concepts for urban buildings with respect to non-urban ones, even though they are, by law, in the same climate zone. Finally, using whole weather data series is important to design the hygrothermal response of buildings to changing climates.

Acknowledgments

This work was initially supported by the Italian Ministry for Education, University and Research (MIUR) with the research grant funding the project PRIN 2009 "SENSE - Smart building ENvelope for Sustainable Urban Environment". A.L. Pisello's acknowledgments are due to the UNESCO Chair "Water Resources Management and Culture", for supporting her research. A.L. Pisello, V.L. Castaldo and F. Cotana want to acknowledge that the research leading to these results has received funding from the European Union's Horizon 2020 research and innovation programme under grant agreements No. 657466 (INPATH-TES) and No. 678407 (ZERO-PLUS). We thank the staff of Osservatorio Meteo Milano Duomo for valuable suggestions and for the validation of weather data of the station used to derive the range tests values.

References

- [1] C. Rosenzweig, W. Solecki, S.A. Hammer, S. Mehrotra, Cities lead the way in climate-change action., *Nature*. 467 (2010) 909–11. doi:10.1038/467909a.
- [2] A.J. Arnfield, Two decades of urban climate research: a review of turbulence, exchanges of energy and water, and the urban heat island, *International Journal of Climatology*. 23 (2003) 1–26. doi:10.1002/joc.859.
- [3] M. Santamouris, On the energy impact of urban heat island and global warming on buildings, *Energy and Buildings*. 82 (2014) 100–113. doi:10.1016/j.enbuild.2014.07.022.
- [4] M.P. McCarthy, M.J. Best, R.A. Betts, Climate change in cities due to global warming and urban effects, *Geophysical Research Letters*. 37 (2010) n/a-n/a. doi:10.1029/2010GL042845.
- [5] T.R. Oke, The energetic basis of the urban heat island, *Quarterly Journal of the Royal Meteorological Society*. 108 (1982) 1–24. doi:10.1002/qj.49710845502.
- [6] M. Kolokotroni, R. Giridharan, Urban heat island intensity in London: An investigation of the impact of physical characteristics on changes in outdoor air temperature during summer, *Solar Energy*. 82 (2008) 986–998. doi:10.1016/j.solener.2008.05.004.
- [7] R. Giridharan, M. Kolokotroni, Urban heat island characteristics in London during winter, *Solar Energy*. 83 (2009) 1668–1682. doi:10.1016/j.solener.2009.06.007.
- [8] M. Santamouris, C. Cartalis, A. Synnefa, Local urban warming, possible impacts and a

- resilience plan to climate change for the historical center of Athens, Greece, *Sustainable Cities and Society*. 19 (2015) 281–291. doi:10.1016/j.scs.2015.02.001.
- [9] D. Mitchell, C. Heaviside, S. Vardoulakis, C. Huntingford, G. Masato, B. P. Guillod, et al., Attributing human mortality during extreme heat waves to anthropogenic climate change, *Environmental Research Letters*. 11 (2016) 74006. doi:10.1088/1748-9326/11/7/074006.
- [10] C.S.B. Grimmond, M. Roth, T.R. Oke, Y.C. Au, M. Best, R. Betts, et al., Climate and more sustainable cities: Climate information for improved planning and management of cities (Producers/Capabilities Perspective), in: *Procedia Environmental Sciences*, 2010: pp. 247–274. doi:10.1016/j.proenv.2010.09.016.
- [11] K.D. Hage, Urban-Rural Humidity Differences, *Journal of Applied Meteorology*. 14 (1975) 1277–1283. doi:10.1175/1520-0450(1975)014<1277:URHD>2.0.CO;2.
- [12] W. Kuttler, S. Weber, J. Schonfeld, A. Hesselschwerdt, Urban/rural atmospheric water vapour pressure differences and urban moisture excess in Krefeld, Germany, *International Journal of Climatology*. 27 (2007) 2005–2015. doi:10.1002/joc.1558.
- [13] T.R. Oke, Street design and urban canopy layer climate, *Energy and Buildings*. 11 (1988) 103–113. doi:10.1016/0378-7788(88)90026-6.
- [14] I. Eliasson, B. Offerle, C.S.B. Grimmond, S. Lindqvist, Wind fields and turbulence statistics in an urban street canyon, *Atmospheric Environment*. 40 (2006) 1–16. doi:10.1016/j.atmosenv.2005.03.031.
- [15] B. Offerle, I. Eliasson, C.S.B. Grimmond, B. Holmer, Surface heating in relation to air temperature, wind and turbulence in an urban street canyon, *Boundary-Layer Meteorology*. 122 (2006) 273–292. doi:10.1007/s10546-006-9099-8.
- [16] J.M. Shepherd, H. Pierce, A.J. Negri, Rainfall Modification by Major Urban Areas: Observations from Spaceborne Rain Radar on the TRMM Satellite, *Journal of Applied Meteorology*. 41 (2002) 689–701. doi:10.1175/1520-0450(2002)041<0689:RMBMUA>2.0.CO;2.
- [17] OECD, *OECD Territorial Reviews: Milan, Italy 2006*, 2006. doi:10.1787/9789264028920-en.
- [18] Comune di Milano, *Sistema Statistico Integrato. Comune di Milano (Statistic Service of Milan's Municipality)*, (2016). <http://sisi.comune.milano.it/> (accessed October 27, 2016).
- [19] P. Bacci, M. Maugeri, The urban heat island of Milan, *Il Nuovo Cimento C*. 15 (1992) 417–424. doi:10.1007/BF02511742.
- [20] R. Anniballe, S. Bonafoni, M. Pichierri, Spatial and temporal trends of the surface and air heat island over Milan using MODIS data, *Remote Sensing of Environment*. 150 (2014) 163–171. doi:10.1016/j.rse.2014.05.005.
- [21] S. Magli, C. Lodi, L. Lombroso, A. Muscio, S. Teggi, Analysis of the urban heat island effects on building energy consumption, *International Journal of Energy and Environmental Engineering*. 6 (2014) 91–99. doi:10.1007/s40095-014-0154-9.
- [22] J. Taylor, P. Wilkinson, M. Davies, B. Armstrong, Z. Chalabi, A. Mavrogianni, et al., Mapping the effects of urban heat island, housing, and age on excess heat-related mortality in London, *Urban Climate*. 14 (2015) 517–528. doi:10.1016/j.uclim.2015.08.001.
- [23] P. Symonds, J. Taylor, A. Mavrogianni, M. Davies, C. Shrubsole, I. Hamilton, et al., Overheating in English dwellings: comparing modelled and monitored large-scale datasets, *Building Research & Information*. (2016) 1–14. doi:10.1080/09613218.2016.1224675.
- [24] P. Michelozzi, F. De Donato, L. Bisanti, A. Russo, E. Cadum, M. De Maria, et al., The impact of the summer 2003 heat waves on mortality in four Italian cities, *Euro*

- Surveillance: Bulletin European Sur Les Maladies Transmissibles= European Communicable Disease Bulletin. 10 (2005) 161–165. <http://www.eurosurveillance.org/images/dynamic/EQ/v05n03/v05n03.pdf>.
- [25] A. Holm, H.M. Kuenzel, K. Sedlbauer, The Hygrothermal Behaviour of Rooms : Combining Thermal Building Simulation and Hygrothermal Envelope Calculation, in: Eighth International Building Performance Simulation Association Conference, Eindhoven, Netherlands, 2003: pp. 499–506. http://www.ibpsa.org/%5Cproceedings%5CBS2003%5CBS03_0499_506.pdf.
- [26] H.M. Künzel, Simultaneous Heat and Moisture Transport in Building Components One- and two-dimensional calculation using simple parameters., Fraunhofer IRB Verlag, Stuttgart, Germany, 1995. http://www.hoki.ibp.fraunhofer.de/ibp/publikationen/dissertationen/hk_dissertation_e.pdf.
- [27] F. Antretter, F. Sauer, T. Schöpfer, A. Holm, Validation of a hygrothermal whole building simulation software, in: 12th Conference of International Building Performance Simulation Association, Sydney, Australia, 2011: pp. 1694–1701. http://www.ibpsa.org/proceedings/bs2011/p_1554.pdf.
- [28] H.M. Künzel, A. Holm, D. Zirkelbach, A.N. Karagiozis, Simulation of indoor temperature and humidity conditions including hygrothermal interactions with the building envelope, Solar Energy. 78 (2005) 554–561. doi:10.1016/j.solener.2004.03.002.
- [29] D. Allinson, M. Hall, Hygrothermal analysis of a stabilised rammed earth test building in the UK, Energy and Buildings. 42 (2010) 845–852. doi:10.1016/j.enbuild.2009.12.005.
- [30] F. Antretter, C. Mitterer, S.M. Young, Use of moisture-buffering tiles for indoor climate stability under different climatic requirements, HVAC and R Research. 18 (2012) 275–282. doi:10.1080/10789669.2012.645399.
- [31] H. Ge, F. Baba, Dynamic effect of thermal bridges on the energy performance of a low-rise residential building, Energy and Buildings. 105 (2015) 106–118. doi:10.1016/j.enbuild.2015.07.023.
- [32] P. Caputo, G. Costa, S. Ferrari, A supporting method for defining energy strategies in the building sector at urban scale, Energy Policy. 55 (2013) 261–270. doi:10.1016/j.enpol.2012.12.006.
- [33] I. Ballarini, S.P. Corgnati, V. Corrado, Use of reference buildings to assess the energy saving potentials of the residential building stock: The experience of TABULA project, Energy Policy. 68 (2014) 273–284. doi:10.1016/j.enpol.2014.01.027.
- [34] Governo Italiano, DM 26 giugno 2015. Applicazione delle metodologie di calcolo delle prestazioni energetiche e definizione delle prescrizioni e dei requisiti minimi degli edifici. (15A05198), (2015) GU Serie Generale n.162 del 15-n.7-n.2015-n.Suppl. Ord.
- [35] R. Paolini, M. Zinzi, T. Poli, E. Carnielo, A.G. Mainini, Effect of ageing on solar spectral reflectance of roofing membranes: natural exposure in Roma and Milano and the impact on the energy needs of commercial buildings, Energy and Buildings. 84 (2014) 333–343. doi:10.1016/j.enbuild.2014.08.008.
- [36] R. Paolini, M. Sleiman, G. Terraneo, T. Poli, M. Zinzi, R. Levinson, et al., Solar spectral reflectance of building envelope materials after natural exposure in Rome and Milano, and after accelerated aging, in: A. Muscio (Ed.), Third International Conference on Countermeasures to Urban Heat Island, Venice, Italy, 2014: pp. 498–509.
- [37] ARPA Lombardia, Weather data, Weather Database. ARPA Lombardia (Environmental Protection Agency of Lombardy Region - Italy). (2016).

- <http://www2.arpalombardia.it/> (accessed October 10, 2015).
- [38] D.T. Reindl, W.A. Beckman, J.A. Duffie, Diffuse fraction correlations, *Solar Energy*. 45 (1990) 1–7. doi:10.1016/0038-092X(90)90060-P.
- [39] F. Lindberg, B. Holmer, S. Thorsson, SOLWEIG 1.0--modelling spatial variations of 3D radiant fluxes and mean radiant temperature in complex urban settings., *International Journal of Biometeorology*. 52 (2008) 697–713. doi:10.1007/s00484-008-0162-7.
- [40] G.J. Levermore, J.B. Parkinson, Analyses and algorithms for new Test Reference Years and Design Summer Years for the UK, *Building Service Engineering Research and Technology*. 27 (2006) 311–325. doi:10.1177/0143624406071037.
- [41] P. Coulibaly, N.D. Evora, Comparison of neural network methods for infilling missing daily weather records, *Journal of Hydrology*. 341 (2007) 27–41. doi:10.1016/j.jhydrol.2007.04.020.
- [42] J. Estévez, P. Gavilán, J.V. Giráldez, Guidelines on validation procedures for meteorological data from automatic weather stations, *Journal of Hydrology*. 402 (2011) 144–154. doi:10.1016/j.jhydrol.2011.02.031.
- [43] OMD, Osservatorio Meteorologico di Milano Duomo, (2016). <http://www.meteoduomo.it/> (accessed April 28, 2016).
- [44] ArcCIS - Archivio Climatologico Italia Settentrionale, Summer Season 2014, 2014. http://www.arcis.it/documenti/ARCIS_jja2014_en.pdf.
- [45] A. Kubilay, D. Derome, B. Blocken, J. Carmeliet, High-resolution field measurements of wind-driven rain on an array of low-rise cubic buildings, *Building and Environment*. 78 (2014) 1–13. doi:10.1016/j.buildenv.2014.04.004.
- [46] M. Abuku, H. Janssen, J. Poesen, S. Roels, Impact, absorption and evaporation of raindrops on building facades, *Building and Environment*. 44 (2009) 113–124. doi:10.1016/j.buildenv.2008.02.001.
- [47] ISO, ISO 13790. Energy performance of buildings - Calculation of energy use for space heating and cooling, (2008).
- [48] K. Kumaran, C. Sanders, Boundary conditions and whole building HAM analysis. Annex 41 MOIST-ENG Subtask 3., 2008.
- [49] K.T. Papakostas, B.A. Sotiropoulos, Occupational and energy behaviour patterns in Greek residences, *Energy and Buildings*. 26 (1997) 207–213. doi:10.1016/S0378-7788(97)00002-9.
- [50] ISO, ISO 13788. Hygrothermal performance of building components and building elements - Internal surface temperature to avoid critical surface humidity and interstitial condensation - Calculation methods, (2012).
- [51] C. Dimitroulopoulou, Ventilation in European dwellings: A review, *Building and Environment*. 47 (2012) 109–125. doi:10.1016/j.buildenv.2011.07.016.
- [52] UK Government, National Calculation Methodology (NCM) modelling guide (for buildings other than dwellings in England and Wales), (2008).
- [53] CEN, EN 15251. Indoor environmental input parameters for design and assessment of energy performance of buildings addressing indoor air quality, thermal environment, lighting and acoustics, (2007).
- [54] ASHRAE, ASHRAE Standard 160-2009. Criteria for Moisture-Control Design Analysis in Buildings., (2009).
- [55] A.L. Pisello, M. Goretti, F. Cotana, A method for assessing buildings' energy efficiency by dynamic simulation and experimental activity, *Applied Energy*. 97 (2012) 419–429. doi:10.1016/j.apenergy.2011.12.094.
- [56] S. Carlucci, L. Pagliano, A review of indices for the long-term evaluation of the general thermal comfort conditions in buildings, *Energy and Buildings*. 53 (2012) 194–

205. doi:10.1016/j.enbuild.2012.06.015.
- [57] S. Attia, S. Carlucci, Impact of different thermal comfort models on zero energy residential buildings in hot climate, *Energy and Buildings*. 102 (2015) 117–128. doi:10.1016/j.enbuild.2015.05.017.
- [58] J.M. Masterton, F.A. Richardson, Humidex, a Method of Quantifying Human Discomfort Due to Excessive Heat and Humidity, (1979).
- [59] S. Conti, P. Meli, G. Minelli, R. Solimini, V. Toccaceli, M. Vichi, et al., Epidemiologic study of mortality during the Summer 2003 heat wave in Italy, *Environmental Research*. 98 (2005) 390–399. doi:10.1016/j.envres.2004.10.009.
- [60] S. Conti, M. Masocco, P. Meli, G. Minelli, E. Palummeri, R. Solimini, et al., General and specific mortality among the elderly during the 2003 heat wave in Genoa (Italy)., *Environmental Research*. 103 (2007) 267–74. doi:10.1016/j.envres.2006.06.003.
- [61] P. Biddulph, D. Crowther, B. Leung, T. Wilkinson, B. Hart, T. Oreszczyn, et al., Predicting the population dynamics of the house dust mite *Dermatophagoides pteronyssinus* (Acari: Pyroglyphidae) in response to a constant hygrothermal environment using a model of the mite life cycle, *Experimental and Applied Acarology*. 41 (2007) 61–86. doi:10.1007/s10493-007-9056-3.
- [62] M.D. Manzar, M. Sethi, M.E. Hussain, Humidity and sleep: a review on thermal aspect, *Biological Rhythm Research*. 43 (2012) 439–457. doi:10.1080/09291016.2011.597621.
- [63] L. Lan, Z. Lian, Ten questions concerning thermal environment and sleep quality, *Building and Environment*. 99 (2016) 252–259. doi:10.1016/j.buildenv.2016.01.017.
- [64] A. V Arundel, E.M. Sterling, J.H. Biggin, T.D. Sterling, Indirect health effects of relative humidity in indoor environments., *Environmental Health Perspectives*. 65 (1986) 351–61. <http://www.pubmedcentral.nih.gov/articlerender.fcgi?artid=1474709&tool=pmcentrez&rendertype=abstract> (accessed January 28, 2016).
- [65] K. Sedlbauer, Prediction of mould fungus formation on the surface of and inside building components, (2001). http://www.hoki.ibp.fhg.de/ibp/publikationen/dissertationen/ks_dissertation_e.pdf.
- [66] E. Vereecken, S. Roels, Review of mould prediction models and their influence on mould risk evaluation, *Building and Environment*. 51 (2012) 296–310. doi:10.1016/j.buildenv.2011.11.003.
- [67] N.L. Nagda, M. Hodgson, Low Relative Humidity and Aircraft Cabin Air Quality, *Indoor Air*. 11 (2001) 200–214. doi:10.1034/j.1600-0668.2001.011003200.x.
- [68] M. Sato, S. Fukayo, E. Yano, Adverse Environmental Health Effects of Ultra-low Relative Humidity Indoor Air, *Journal of Occupational Health*. 45 (2003) 133–136. doi:10.1539/joh.45.133.
- [69] P. Wolkoff, S.K. Kjaergaard, The dichotomy of relative humidity on indoor air quality., *Environment International*. 33 (2007) 850–7. doi:10.1016/j.envint.2007.04.004.
- [70] M. Ucci, P. Biddulph, T. Oreszczyn, D. Crowther, T. Wilkinson, S.E.C. Pretlove, et al., Application of a transient hygrothermal population model for house dust mites in beds: assessment of control strategies in UK buildings, *Journal of Building Performance Simulation*. 4 (2011) 285–300. doi:10.1080/19401493.2010.532235.
- [71] A. Fouillet, G. Rey, F. Laurent, G. Pavillon, S. Bellec, C. Guihenneuc-Jouyau, et al., Excess mortality related to the August 2003 heat wave in France, *International Archives of Occupational and Environmental Health*. 80 (2006) 16–24. doi:10.1007/s00420-006-0089-4.
- [72] J.C. Semenza, C.H. Rubin, K.H. Falter, J.D. Selanikio, W.D. Flanders, H.L. Howe, et

- al., Heat-Related Deaths during the July 1995 Heat Wave in Chicago, *New England Journal of Medicine*. 335 (1996) 84–90. doi:10.1056/NEJM199607113350203.
- [73] K.M.A. Gabriel, W.R. Endlicher, Urban and rural mortality rates during heat waves in Berlin and Brandenburg, Germany, *Environmental Pollution*. 159 (2011) 2044–2050. doi:10.1016/j.envpol.2011.01.016.
- [74] G. Rey, E. Jouglu, A. Fouillet, G. Pavillon, P. Bessemoulin, P. Frayssinet, et al., The impact of major heat waves on all-cause and cause-specific mortality in France from 1971 to 2003., *International Archives of Occupational and Environmental Health*. 80 (2007) 615–26. doi:10.1007/s00420-007-0173-4.
- [75] M. Kato, B.G. Phillips, G. Sigurdsson, K. Narkiewicz, C.A. Pesek, V.K. Somers, Effects of sleep deprivation on neural circulatory control., *Hypertension*. 35 (2000) 1173–1175. doi:10.1161/01.HYP.35.5.1173.
- [76] P. Heslop, G.D. Smith, C. Metcalfe, J. Macleod, C. Hart, Sleep duration and mortality: the effect of short or long sleep duration on cardiovascular and all-cause mortality in working men and women, *Sleep Medicine*. 3 (2002) 305–314. doi:10.1016/S1389-9457(02)00016-3.
- [77] D.F. Kripke, L. Garfinkel, D.L. Wingard, M.R. Klauber, M.R. Marler, J. EO, et al., Mortality Associated With Sleep Duration and Insomnia, *Archives of General Psychiatry*. 59 (2002) 131. doi:10.1001/archpsyc.59.2.131.
- [78] J.C. Semenza, J.E. McCullough, W.D. Flanders, M.A. McGeehin, J.R. Lumpkin, Excess hospital admissions during the July 1995 heat wave in Chicago, *American Journal of Preventive Medicine*. 16 (1999) 269–277. doi:10.1016/S0749-3797(99)00025-2.
- [79] R. Paolini, A.G. Mainini, T. Poli, L. Vercesi, Assessment of Thermal Stress in a Street Canyon in Pedestrian Area with or without Canopy Shading, *Energy Procedia*. 48 (2014) 1570–1575. doi:10.1016/j.egypro.2014.02.177.
- [80] S. Saneinejad, P. Moonen, J. Carmeliet, Coupled CFD, radiation and porous media model for evaluating the micro-climate in an urban environment, *Journal of Wind Engineering and Industrial Aerodynamics*. 128 (2014) 1–11. doi:10.1016/j.jweia.2014.02.005.
- [81] F. Haldi, D. Robinson, Interactions with window openings by office occupants, *Building and Environment*. 44 (2009) 2378–2395. doi:10.1016/j.buildenv.2009.03.025.
- [82] X. Xu, J.E. Taylor, A.L. Pisello, Network synergy effect: Establishing a synergy between building network and peer network energy conservation effects, *Energy and Buildings*. 68 (2014) 312–320. doi:10.1016/j.enbuild.2013.09.017.
- [83] L.C. Tagliabue, M. Manfren, A.L.C. Ciribini, E. De Angelis, Probabilistic behavioural modeling in building performance simulation—The Brescia eLUX lab, *Energy and Buildings*. 128 (2016) 119–131. doi:10.1016/j.enbuild.2016.06.083.